

Title	Self-limiting processes in thermal atomic layer etching of nickel by hexafluoroacetylacetone
Author(s)	Basher, Abdulrahman H.; Hamada, Ikutaro; Hamaguchi, Satoshi
Citation	Japanese Journal of Applied Physics. 59(9) p.090905
Issue Date	2020-09
oaire:version	VoR
URL	<a href="https://hdl.handle.net/11094/78315">https://hdl.handle.net/11094/78315</a>
rights	© 2020 The Japan Society of Applied Physics. This article is licensed under a Creative Commons Attribution 4.0 International License.
Note	

***Osaka University Knowledge Archive : OUKA***

<https://ir.library.osaka-u.ac.jp/>

Osaka University

RAPID COMMUNICATION • OPEN ACCESS

## Self-limiting processes in thermal atomic layer etching of nickel by hexafluoroacetylacetone

To cite this article: Abdulrahman H. Basher *et al* 2020 *Jpn. J. Appl. Phys.* **59** 090905

View the [article online](#) for updates and enhancements.



# Self-limiting processes in thermal atomic layer etching of nickel by hexafluoroacetylacetone

Abdulrahman H. Basher<sup>1\*</sup>, Ikutaro Hamada<sup>2</sup>, and Satoshi Hamaguchi<sup>1\*</sup>

<sup>1</sup>Center for Atomic and Molecular Technologies, Osaka University, Osaka, Japan

<sup>2</sup>Department of Precision Engineering, Graduate School of Engineering, Osaka University, Osaka, Japan

\*E-mail: [a.h.basher@ppl.eng.osaka-u.ac.jp](mailto:a.h.basher@ppl.eng.osaka-u.ac.jp); [hamaguch@ppl.eng.osaka-u.ac.jp](mailto:hamaguch@ppl.eng.osaka-u.ac.jp)

Received July 6, 2020; revised July 21, 2020; accepted July 26, 2020; published online August 18, 2020

In thermal atomic layer etching (ALE) of Ni, a thin oxidized Ni layer is removed by a hexafluoroacetylacetone (hfach) etchant gas at an elevated surface temperature, and etching ceases when a metallic Ni surface appears (self-limiting step). However, atomistic details of the self-limiting step was not well understood. With periodic density-functional-theory calculations, it is found that hfach molecules barrierlessly adsorb and tend to decompose on a metallic Ni surface, in contrast to the case of a NiO surface, where they can form volatile Ni(hfac)<sub>2</sub>. Our results clarify the origin of the self-limiting process in the thermal ALE. © 2020 The Japan Society of Applied Physics

Atomic layer etching (ALE) is a processing technology to perform cyclic removal of a monolayer (or a few monolayers) of a material surface at one time in a controlled manner. It is considered to be one of the most promising etching technologies for nano-scale electronic devices.<sup>1–8</sup> As in atomic layer deposition,<sup>8–12</sup> there is a self-limiting step<sup>9–11,13</sup> in ALE, which allows the removal of no more than a single monolayer (or a few monolayers) of the material at one time. The goal of this paper is to present the self-limiting mechanism of thermal ALE of Ni. Analogous mechanisms are considered operational for similar ALE processes of other metals.

Thermal ALE of nickel (Ni) may be performed in the following manner: first, the surface of a Ni film is modified to form a thin nickel oxide (NiO) layer. Second, the film is exposed to a hexafluoroacetylacetone (hfach) gas at an elevated temperature of 300 ~ 400 °C. In this step, volatile nickel hexafluoroacetylacetonate Ni(hfac)<sub>2</sub> is formed and desorb until the NiO layer is exhausted. When a metallic Ni surface appears, etching ceases self-limitingly even if the surface is continued to be exposed to hfach. The cycle of the oxidation and NiO removal steps are repeated until the etching of a desired depth is achieved.<sup>14–16</sup>

It is experimentally known that Ni(hfac)<sub>2</sub> is formed when a NiO surface is exposed to hfach at elevated temperature.<sup>14,17</sup> Earlier studies<sup>15,16</sup> by Basher et al. clarified the reaction mechanisms for deprotonation of hfach on a NiO surface and possible formation of Ni(hfac)<sub>2</sub>, using density functional theory (DFT) calculations. It is also experimentally known that, when a metallic Ni surface is exposed to hfach, hfach molecules typically decompose on the surface, without forming Ni(hfac)<sub>2</sub>. In this study, we clarify the adsorption and decomposition mechanisms of hfach on a metallic Ni surface, using DFT calculations.

All DFT calculations in this work were performed with our in-house code STATE.<sup>18,19</sup> We used ultra-soft pseudopotentials<sup>20</sup> to describe electron-ion interactions. Wave functions and augmentation charge were expanded in terms of a plane-wave basis set with the cutoff energies of 36 Ry and 400 Ry, respectively. Spin polarization was taken into account. The rev-vdW-DF2<sup>21,22</sup> functional was used as the exchange-correlation functional. The Ni surface material

was modeled with the (4 × 4) surface unit cell in the horizontal direction and with a four-atomic-layer thick slab and a vacuum equivalent to sixteen atomic layers in the vertical direction. The slab was constructed with the lattice constant of Ni obtained from the calculation using the rev-vdW-DF2 functional. The surface Brillouin zone was sampled with a 2 × 2 k-point set. An hfach molecule was deposited on one side of the slab, and the artificial electrostatic interaction among the image slabs was eliminated by the effective screening medium method.<sup>23,24</sup> Reaction pathways were investigated by using the climbing image nudged elastic band (CINEB) method.<sup>25,26</sup>

As in earlier studies,<sup>15,16</sup> enol hfach<sup>27,28</sup> was used as an incident molecule in this study. We first studied the adsorption state of an hfach molecule on the low index Ni surfaces, i.e. (100), (110), and (111) surfaces. An hfach molecule was systematically placed and optimized on various sites in different orientations on these surfaces. We then evaluated the adsorption energy defined by  $E_{\text{ads}} = E_{\text{tot}}(\text{hfach}/\text{Ni}) - E_{\text{tot}}(\text{Ni}) - E_{\text{tot}}(\text{hfach})$ , where  $E_{\text{tot}}(\text{hfach}/\text{Ni})$ ,  $E_{\text{tot}}(\text{Ni})$ , and  $E_{\text{tot}}(\text{hfach})$ , are the total energies of the hfach adsorbed Ni surface material model (which we call the “adsorption system”), the Ni surface material model, and the isolated hfach molecule, respectively. The structures of all systems were optimized. The lowest adsorption energy on each surface was  $E_{\text{ads}} = -0.64$  eV,  $-1.19$  eV, or  $-0.42$  eV for the (100), (110), or (111) surface, respectively. In the most stable adsorption configuration, hfach adsorbs in the upright configuration with its oxygen atoms pointing toward the surface regardless of the surface orientation [See Fig. 1(a) for the adsorption geometry on Ni(110)]. We also studied the adsorption state of hfach on Ni(110) with the Perdew–Burke–Ernzerhof (PBE)<sup>29,30</sup> functional and obtained the adsorption energy of  $-0.41$  eV, which was much smaller than that obtained with rev-vdW-DF2. Because the PBE functional cannot describe the dispersion force properly, we conclude that hfach physisorbed (adsorbed mostly due to the dispersion force or what is roughly known as van der Waals force) on the surface in the case of Fig. 1(a). The fact that  $E_{\text{ads}}$  for the (110) surface is the lowest suggests that this surface is the most reactive among those considered in this work, which is in agreement with previous studies.<sup>31,32</sup> Therefore, in what follows, we focus only on Ni(110) as a representative surface.



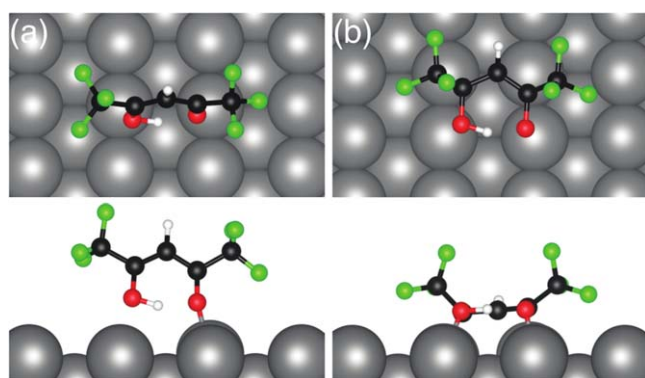


**Fig. 1.** (Color online) Top (upper) and side (lower) views of atomic geometry of an hfach molecule (a) physisorbed or (b) chemisorbed on a Ni(110) surface. Here H, C, O, F, and Ni atoms are indicated by white, black, red, green, and gray spheres, respectively.

We further explored possible chemisorption states on Ni(110). By changing the molecular orientation of the most stable physisorption state of Fig. 1(a), we found a thermodynamically more stable state at  $E_{\text{ads}} = -2.08$  eV, where the hfach molecule is in a side-on configuration with the C–O–Ni angle of around  $90^\circ$ , as shown in Fig. 1(b). Figure 2 shows the charge density difference for Fig. 1(b), which is defined by  $\Delta\rho = \rho_{\text{ads}} - \rho_{\text{hfach}} - \rho_{\text{Ni}}$ . Here  $\rho_{\text{ads}}$  denotes the electron density of the adsorption system, and  $\rho_{\text{hfach}}$  and  $\rho_{\text{Ni}}$  denote those of the isolated hfach molecule and the Ni surface material model in their adsorption geometries. It is seen that the electron (i.e. negative) charges are accumulated between C atoms of hfach and Ni atoms underneath, which indicates the formation of covalent-like bonds. We also performed the crystal orbital overlap analysis<sup>33,34</sup> and found that the occupied molecular orbitals interact repulsively with

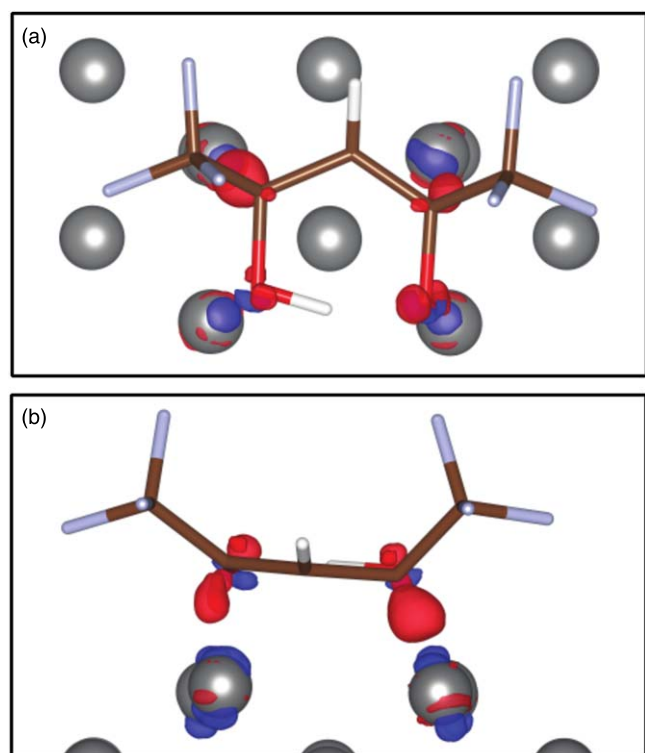


**Fig. 2.** (Color online) (a) Top and (b) side views of the charge density difference of hfach on Ni(110). The red (blue) isosurface indicates negative (positive) charge accumulation.

the substrate states, while the lowest unoccupied molecular orbital (LUMO) and the next LUMO hybridize with the substrate state. These observations indicate that the adsorption state of Fig. 1(b) is chemisorption.

Our calculations show that physisorption and chemisorption steps of Fig. 1 occur barrierlessly, indicating that hfach molecules adsorb on a metallic Ni surface at zero temperature. We now study whether such adsorbed hfach possibly form Ni(hfac)<sub>2</sub> at elevated temperature. The first step toward the formation of Ni(hfac)<sub>2</sub> is deprotonation or the removal of hydrogen (H) atom from hfach, so that the O atoms of an hfach molecule can directly bond with a surface Ni atom. By placing an hfach molecule sufficiently close to the Ni (110) surface and performing structural optimization, we obtained a stable deprotonated state whose adsorption energy is  $E_{\text{ads}} = -1.82$  eV. We then performed the reaction path search with the CINEB method between the chemisorbed state of Fig. 1(b) and this deprotonated state. The calculated energy profile is plotted in Fig. 3(a) along with the atomic geometries of the initial (IS), transition (TS), and final (FS) states. The initial state is prior to the hfach–Ni interaction and the final state is the deprotonated state. The chemisorbed state is denoted by hfach\* in Fig. 3. The calculated activation barrier was found to be 1.09 eV.

Similarly by placing an hfach molecule sufficiently close to the Ni surface at different locations and performing structural optimization, we obtained a state of hfach dissociation with  $E_{\text{ads}} = -2.65$  eV, where one of its F atoms is bonded with a Ni atom on the surface, i.e. the hfach is decomposed by defluorination. We then performed a CINEB

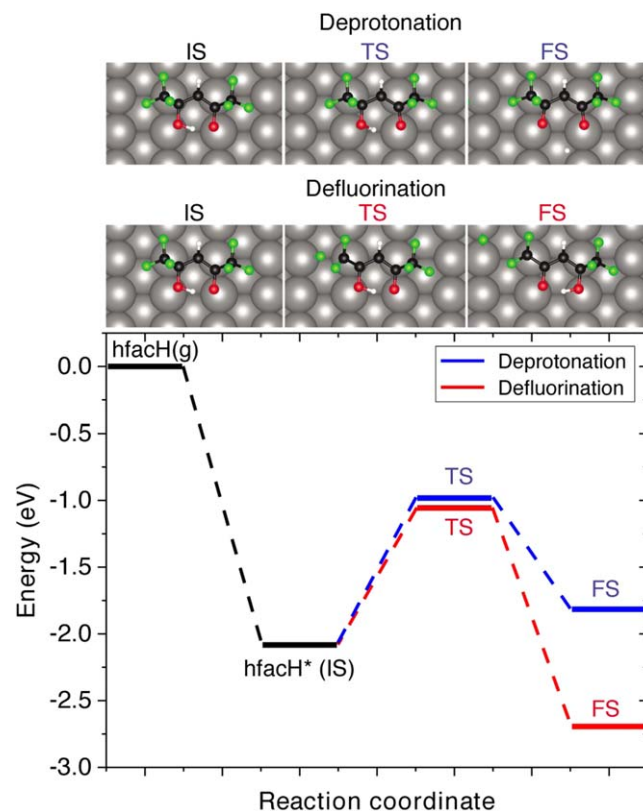


**Fig. 3.** (Color online) Energy profiles for deprotonation and C–F bond dissociation (defluorination) of hfach on Ni(110). Top views of the atomic geometries for the initial (IS), transition (TS), and final (FS) states for deprotonation (upper) and defluorination (lower) are shown above the energy profiles.

calculation between the same chemisorbed state and this state of hfacH defluorination. The calculated energy profile is plotted in Fig. 3. The calculated activation barrier was found to be 1.02 eV, similar to that for deprotonation as discussed above. These energy profiles indicate that chemisorbed hfacH molecules on a Ni(110) surface may deprotonate or decompose at higher temperature by overcoming the activation barriers. However, the adsorption energy of the decomposed hfacH molecule on a Ni surface via defluorination is lower than that of the deprotonated hfacH, indicating that the decomposed hfacH by defluorination is thermodynamically more stable. Our finding is in line with earlier experiments,<sup>14,17)</sup> where various decomposed products of hfacH were observed. (Note that our study has not ruled out the possibility of decomposition of hfacH by fragmentation other than defluorination on a metallic Ni surface.) Based on these results, we conclude that hfacH molecules adsorbed on a metallic Ni surface are more likely to decompose via defluorination eventually, rather than to deprotonate and possibly form Ni(hfac)<sub>2</sub> molecule at an elevated surface temperature.

In conclusion, the adsorption and surface reactions of hfacH on a metallic Ni surface has been investigated by using DFT calculations. The reaction paths of hfacH on a metallic Ni that we found are consistent with earlier experimental observations<sup>14,17)</sup> and explain why a self-limiting step occurs in thermal ALE of Ni. As shown in the earlier studies,<sup>15,16)</sup> on a NiO surface, an hfacH molecule barrierlessly deprotonates and forms stable bonds between a surface Ni atom and the deprotonated hfacH, creating precursors for volatile Ni(hfac)<sub>2</sub>. This is because the highly polarized deprotonated hfacH anion interacts electrostatically with the surface charges of the ionically bonded NiO. At a higher surface temperature, desorption of Ni(hfac)<sub>2</sub> and H<sub>2</sub>O from the surface causes etching of the NiO surface. On the other hand, on a metallic Ni surface, hfacH molecules adsorb and tend to decompose without forming volatile Ni(hfac)<sub>2</sub>, as shown in this study. Therefore, in thermal ALE of Ni, when a thin NiO layer is completely removed by hfacH exposure and a metallic Ni surface appears, incident hfacH molecules just adsorb and possibly decompose on the surface without etching the surface. This is the self-limit mechanism of thermal ALE of Ni.

**Acknowledgments** We are grateful to Professor Yoshitada Morikawa of Osaka University for fruitful discussion. This work was partially supported by the Japan Society of the Promotion of Science (JSPS) Grants-in-Aid for Scientific Research (S) (No. 15H05736) and for Scientific Research on Innovative Areas “Hydrogenomics” (No. JP18H05519), as well as JSPS Core-to-Core Program JPJSCCA2019002. Numerical calculations were performed at the Supercomputer Center, Institute for Solid State Physics, University of Tokyo.

**ORCID iDs** Abdulrahman H. Basher  <https://orcid.org/0000-0002-3141-0016> Ikutaro Hamada  <https://orcid.org/0000-0001-5112-2452> Satoshi Hamaguchi  <https://orcid.org/0000-0001-6580-8797>

- 1) S. Rauf, T. Sparks, P. L. G. Ventzek, V. V. Smirnov, A. V. Stengach, K. G. Gaynullin, and V. A. Pavlovsky, *J. Appl. Phys.* **101**, 033308 (2007).
- 2) A. Agarwal and M. J. Kushner, *J. Vac. Sci. Technol. A* **27**, 37 (2009).
- 3) D. Metzler, R. L. Bruce, S. Engelmann, E. A. Joseph, and G. S. Oehrlein, *J. Vac. Sci. Technol. A* **32**, 020603 (2014).
- 4) K. J. Kanarik, T. Lill, E. A. Hudson, S. Sriraman, S. Tan, J. Marks, V. Vahedi, and R. A. Gottscho, *J. Vac. Sci. Technol. A* **33**, 020802 (2015).
- 5) I. Adamovich et al., *J. Phys. D* **50**, 323001 (2017).
- 6) G. S. Oehrlein and S. Hamaguchi, *Plasma Sources Sci. Technol.* **27**, 023001 (2018).
- 7) K. J. Kanarik, S. Tan, and R. A. Gottscho, *J. Phys. Chem. Lett.* **9**, 4814 (2018).
- 8) W. Xie and G. N. Parsons, *J. Vac. Sci. Technol. A* **38**, 022605 (2020).
- 9) S. M. George, *Chem. Rev.* **110**, 111 (2010).
- 10) G. Yuan, N. Wang, S. Huang, and J. Liu, “A brief overview of atomic layer deposition and etching in the semiconductor processing,” 2016 17th Int. Conf. Electron. Packag. Technol. (ICEPT, Wuhan, China, 2016), (2016), p. 1365.
- 11) P. C. Lemaire and G. N. Parsons, *Chem. Mater.* **29**, 6653 (2017).
- 12) H. Li, T. Ito, K. Karahashi, M. Kagaya, T. Moriya, M. Matsukuma, and S. Hamaguchi, *Jpn. J. Appl. Phys.* **59**, SJJA01 (2020).
- 13) A. Fischer, A. Routzahn, Y. Lee, T. Lill, and S. M. George, *J. Vac. Sci. Technol. A* **38**, 022603 (2020).
- 14) T. Ito, K. Karahashi, and S. Hamaguchi, Proc. of the 39th Int. Symp. on Dry Process (DPS2017) (Tokyo, Japan, 2017) 45, 2017.
- 15) A. H. Basher, M. Krstić, T. Takeuchi, M. Isobe, T. Ito, M. Kiuchi, K. Karahashi, W. Wenzel, and S. Hamaguchi, *J. Vac. Sci. Technol. A* **38**, 022610 (2020).
- 16) A. H. Basher, M. Krstić, F. Karin, T. Ito, K. Karahashi, W. Wenzel, and S. Hamaguchi, *J. Vac. Sci. Technol. A* **38**, 052602 (2020).
- 17) H. L. Nigg and R. I. Masel, *J. Vac. Sci. Technol. A* **17**, 3477 (1999).
- 18) Y. Morikawa, H. Ishii, and K. Seki, *Phys. Rev. B* **69**, 041403 (2004).
- 19) Y. Hamamoto, I. Hamada, K. Inagaki, and Y. Morikawa, *Phys. Rev. B* **93**, 245440 (2016).
- 20) D. Vanderbilt, *Phys. Rev. B* **41**, 7892 (1990).
- 21) I. Hamada, *Phys. Rev. B* **89**, 121103 (2014).
- 22) M. Callsen and I. Hamada, *Phys. Rev. B* **91**, 195103 (2015).
- 23) M. Otani and O. Sugino, *Phys. Rev. B* **73**, 115407 (2006).
- 24) I. Hamada, M. Otani, O. Sugino, and Y. Morikawa, *Phys. Rev. B* **80**, 165411 (2009).
- 25) H. Jónsson, G. Mills, and K. W. Jacobsen, in *Classical and Quantum Dynamics in Condensed Phase Simulations*, ed. B. J. Berne, G. Ciccotti, and D. F. Coker (World Scientific, Singapore, 1998), p. 385.
- 26) G. Henkelman, B. P. Uberuaga, and H. Jónsson, *J. Chem. Phys.* **113**, 9901 (2000).
- 27) K. Manbeck, N. Boaz, N. Bair, A. Sanders, and A. Marsh, *J. Chem. Educ.* **88**, 1444 (2011).
- 28) S. Engmann, B. Ómarsson, M. Lacko, M. Stano, Š. Matejček, and O. Ingólfsson, *J. Chem. Phys.* **138**, 234309 (2013).
- 29) J. P. Perdew, K. Burke, and M. Ernzerhof, *Phys. Rev. Lett.* **77**, 3865 (1996).
- 30) J. P. Perdew, K. Burke, and M. Ernzerhof, *Phys. Rev. Lett.* **78**, 1396 (1997).
- 31) H. Seenivasan and A. K. Tiwari, *J. Chem. Phys.* **140**, 174704 (2014).
- 32) H. Seenivasan, B. Jackson, and A. K. Tiwari, *J. Chem. Phys.* **146**, 074705 (2017).
- 33) R. Hoffmann, *Rev. Mod. Phys.* **60**, 601 (1988).
- 34) H. Aizawa and S. Tsuneyuki, *Surf. Sci.* **399**, L364 (1998).